

1D Frequency Transformation- Based Amplitude- Only Images for Copyright- and Privacy- Protection in Image Trading Systems

Wannida Sae-Tang¹, Shenchuan Liu²,
Masaaki Fujiyoshi³, and Hitoshi Kiya⁴, Non-members

ABSTRACT

This paper proposes an effective method of generating amplitude-only images (AOIs) which are inversely transformed amplitude components of images and which are used in the copyright- and privacy-protected digital fingerprinting-based image trading systems. The proposed method applies a one-dimensional frequency transformation to an image for generating the AOI with low intensity range (IR), whereas the IR of the AOI in the conventional method using a two-dimensional transformation is too large to store or transmit. The proposed method is distinct from other IR reduction approaches such as clipping, linear and non-linear scaling, block division, and random sign assignment which require extra-calculations, it reduces the computational complexity while it reduces IRs of AOIs. Moreover, experimental results show that the proposed method enhances the quality of fingerprinted images and fingerprinting performance.

Keywords: Discrete Fourier Transformation, Discrete Cosine Transformation, Quantization, Random Sign Assignment, Image Copyright Protection, Image Privacy

1. INTRODUCTION

In image trading systems, the copyright of commercial images should be protected. So, a digital fingerprint which indicates the corresponding consumer is embedded to a purchased image before sending the image to the consumer [1, 2]. Digital fingerprinting is desired to be performed by a trusted third party (TTP) instead of the content provider (CP) for consumers privacy protection, because the CP is not always trustful. Thus, an original image is sent from the CP to the TTP for fingerprinting before sending to the consumer [3]. However, the image sent to the TTP is visible that makes the consumers privacy lost

again. In order to protect both the image copyright and consumers privacy, other image trading systems were proposed [46] where an original image is divided into two parts; one of them is invisible and is sent to the TTP for fingerprinting before being sent to the consumer. Finally, the image copyright and consumers privacy are all protected.

In [6], discrete Fourier transformation (DFT) which is a well-known frequency analysis tool is used to divide the original image into two parts. By applying the DFT to an image, phase and amplitude components are obtained. The inversely discrete Fourier transformed (IDFTed) amplitude components which is called amplitude-only image (AOI) was proposed in [6] for the copyright- and privacy-protection because of its invisibility. On contrary, phase-only image (POI) which is the IDFTed phase components is visible. So, it is used for image reconstruction in the image trading system [6] as similar as in [711]. In other words, the invisible AOI is sent from the CP to the TTP for fingerprinting, and the POI is sent directly from the CP to the consumer as a key for reconstructing the purchased image.

The AOI, however, is the summation of coherent phase cosine signals with various amplitudes and frequencies, so its intensity range (IR) is quite wide comparing to that of the original image. In addition, the histogram of the AOI is skew right with high peak. In order to reduce the IR of the AOI, applying clipping and rounding, or linear or non-linear scaling directly to the AOI can be considered, but these approaches introduce numerous errors due to eliding the skewness of the histogram. Therefore, other IR reduction methods such as block division (BD) [12] and random sign assignment (RSA) [13] were considered. BD divides the original image into sub-images before generating the AOI. It reduces IRs of AOIs and also reduces computational resources. However, the invisibility of the AOI is destroyed by the BD. While, RSA which makes phases of cosine waves incoherent is an effective IR reduction method, but it needs an extra computation [13]. Moreover, DFT was used in [13], so the POI is required to be quantized as well as the AOI, and this also introduces quantization errors to the POI which degrade the quality of the image reconstructed by the consumer.

Manuscript received on September 30, 2013 ; revised on January 8, 2014.

Final manuscript received February 24, 2014.

^{1,2,3,4} The authors are with Department of Information and Communication Systems, Tokyo Metropolitan University, Japan. E-mail: saetang-wannida@ed.tmu.ac.jp, liu-shenchuan@ed.tmu.ac.jp, fujiyoshi-masaaki@tmu.ac.jp, kiya@tmu.ac.jp.

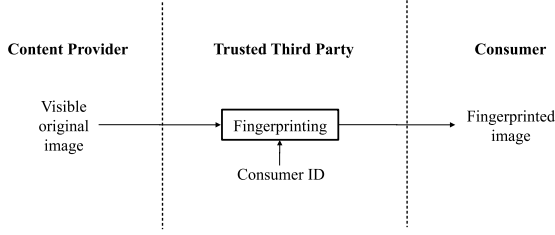


Fig.1: The ordinary copyright-protected image trading system without consumer's privacy protection [3].

To solve the problems mentioned above, one-dimensional discrete cosine transformation (1D DCT)-based AOI was proposed [14]. It reduces the computational complexity as well as IRs of AOIs, whereas the RSA requires an extra calculation. Moreover, the quality of fingerprinted images and fingerprinting performance were significantly enhanced. However, the method has not been well studied yet. In this paper, all considerable conditions for the desired image trading system are focused on. Not only 1D DCT-based AOI, but also 1D DFT-based AOI is proposed in this paper. It is noted that other frequency transformations could be applied. It is clarified how 1D transformation-based image trading system reduces IRs of AOIs significantly. Moreover, it is clarified that the proposed method reduces IRs of AOIs with keeping the invisibility of AOIs, whereas BD destroys the invisibility of the AOIs which are shown in an experimental result part. Dimensions and types of transformations are described and evaluated in turn in this paper. In addition, other IR reduction methods, i.e., clipping and linear scaling are considered and evaluated in this paper for the first time.

The rest of this paper is organized as follows. Section 2 presents the image trading system including the conventional methods [6, 13], and it also describes requirements for the desired image trading system. Section 3 proposes 1D frequency transformation-based AOI, and it describes benefits of the proposed method. It further distinguishes the proposed method from other approaches. Experimental results are given in Section 4. Finally, Section 5 concludes this paper.

2. PRELIMINARIES

This section introduces image trading systems and describes the requirements for the desired image trading system.

2.1 Image Trading Systems

Figure 1 shows the ordinary copyright-protected image trading system [3] without consumers privacy protection. In this system, the image that is sent to the trusted third party (TTP) for fingerprinting is visible. While Figure 2 shows the copyright- and

privacy-protected image trading systems [46, 1214]. In this system, the image sent to the TTP is invisible, therefore, the consumers privacy is protected in addition to copyright protection of images. In this paper, copyright- and privacy-protected image trading system is considered.

2.2 Image Trading System Using Amplitude-Only Images

Figure 3 shows the image trading system using amplitude-only images (AOIs) [6]. In this framework, 2D DFT is used to transform the image to the frequency domain. Let $F(u, v)$ be the $X \times Y$ -sized 2D DFTed coefficients of $X \times Y$ -sized image $f(x, y)$, where $x = 0, 1, \dots, X-1$, $y = 0, 1, \dots, Y-1$, $u = 0, 1, \dots, X-1$, and $v = 0, 1, \dots, Y-1$;

$$F(u, v) = \sum_{x=0}^{X-1} \sum_{y=0}^{Y-1} f(x, y) \exp \left(-j2\pi \left(\frac{ux}{X} + \frac{vy}{Y} \right) \right), \quad (1)$$

where j denotes $\sqrt{-1}$. DFT coefficients $F(u, v)$ can be expressed in the polar form as

$$F(u, v) = |F(u, v)| \exp(j\phi(u, v)), \quad (2)$$

where $|F(u, v)|$ and $\exp(j\phi(u, v))$ denote the amplitude and phase components of $F(u, v)$, respectively. The AOI which is denoted as $A(x, y)$ is obtained by applying 2D IDFT to the amplitude components $|F(u, v)|$ as

$$A(x, y) = \frac{1}{XY} \sum_{u=0}^{X-1} \sum_{v=0}^{Y-1} |F(u, v)| \exp \left(j2\pi \left(\frac{ux}{X} + \frac{vy}{Y} \right) \right). \quad (3)$$

Similarly, the phase-only image (POI) can be defined by applying IDFT to phase components $\exp(j\phi(u, v))$ as

$$P(x, y) = \frac{1}{XY} \sum_{u=0}^{X-1} \sum_{v=0}^{Y-1} \exp(j\phi(u, v)) \exp \left(j2\pi \left(\frac{ux}{X} + \frac{vy}{Y} \right) \right), \quad (4)$$

where $P(x, y)$ denotes the POI.

Figures 4 (a), (b), and (c) show image "Lena," its 2D DFT-based AOI, and its 2D DFT-based POI, respectively. The 2D DFT-based AOI is invisible, but the 2D DFT-based POI reveals the original image. Hence, the 2D DFT-based AOI is sent to the TTP for fingerprinting, and the 2D DFT-based POI is directly sent to the consumer in the image trading system [6]. The consumer can obtain the fingerprinted image by firstly reconstructing amplitude components and phase components of the image by applying 2D DFT to the AOI and the POI, respectively. Then, the fingerprinted image is constructed by applying 2D IDFT to the combination of the reconstructed amplitude and phase components.

However, this system is not practical, because the

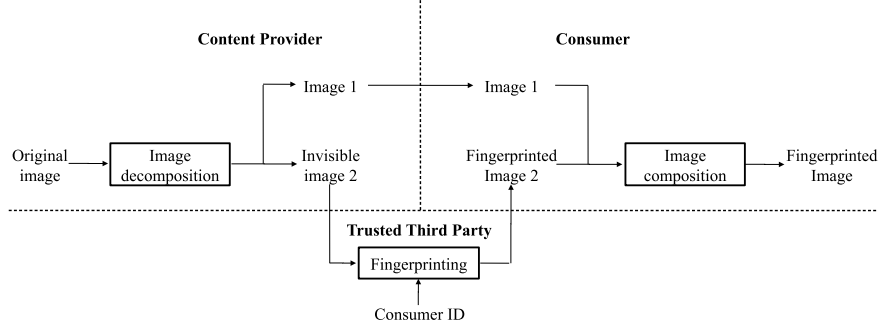


Fig. 2: The copyright- and privacy-protected image trading systems [4-6, 12-14].

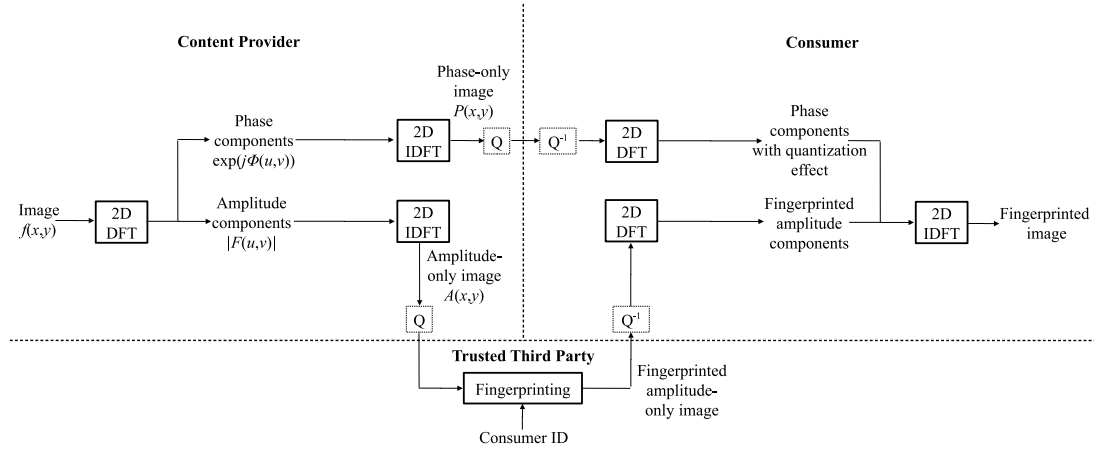


Fig. 3: The image trading system using AOIs [6] (Q : quantization and Q^{-1} : inverse quantization).

AOI and the POI include real numbers. It is impossible to store them in desired bit depths. Therefore, a quantization should be introduced. In addition, intensity ranges (IRs) of both AOI and POI should be considered. The IR of the AOI which this paper focuses on is its interval of pixel intensities, i.e., $[\min(A(x, y)), \max(A(x, y))]$. The IR width which is the length of the interval is given by Eq. (5).

$$\text{IRW} = \max(A(x, y)) - \min(A(x, y)), \quad (5)$$

where IRW denotes the IR width. It is noted that the same definition is applied to the POI. The AOI has quite wide IR width. The IR width of the 2D DFT-based AOI for “Lena” is about twenty times wider than that of the original image as shown in Figure 4. It makes the storage and transmission of AOIs difficult. Huge amounts of memory, high bandwidth, and high computational costs are required. By directly quantizing the AOI to 8 bits per pixel (bpp), numerous quantization errors are occurred, because the histogram of the AOI is skew as shown in Figure 4 (f).

2.3 Image Trading System Using Amplitude-Only Images with Random Sign Assignment

To reduce the quantization errors, the system with random sign assignment (RSA) [13] was proposed to reduce IRs of AOIs before quantization, as shown in Figure 5. RSA symmetrically multiplies random signs to amplitude components $|F(u, v)|$ to reduce the IR of AOI $A(x, y)$ as

$$F'(u, v) = r(u, v)|F(u, v)|, \quad (6)$$

where $F'(u, v)$ which include real numbers are the amplitude components with symmetric random signs, and $r(u, v)$ are random signs, i.e., $r(u, v)$ can either be -1 or 1 . Thus, modified AOI $A'(x, y)$ is obtained as

$$A'(x, y) = \frac{1}{XY} \sum_{u=0}^{X-1} \sum_{v=0}^{Y-1} F'(u, v) \exp\left(j2\pi\left(\frac{ux}{X} + \frac{vy}{Y}\right)\right). \quad (7)$$

That is, the amplitude components are randomly multiplied by -1 or 1 in RSA. In other words, some of cosine waves are randomly shifted by π radian so that the IR of the AOI is reduced. As a result, the quantization error is reduced [13].

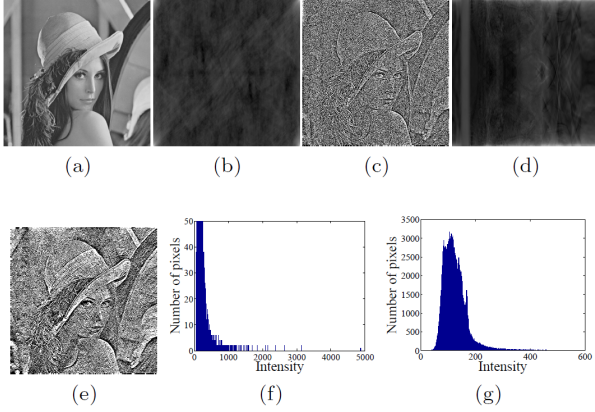


Fig.4: AOIs and POIs; (a) original image $f(x, y)$ (IR width: 255), (b) 2D DFT-based AOI $A(x, y)$ in \ln scale (IR width: 4819.2), (c) 2D DFT-based POI $P(x, y)$, (d) column-wise 1D DFT-based AOI $A_c(x, y)$ (IR width: 520.1), (e) column-wise 1D DFT-based POI $P_c(x, y)$, (f) histogram of 2D DFT-based AOI $A(x, y)$, and (g) histogram of column-wise 1D DFT-based AOI $A_c(x, y)$.

2.4 Requirements for Desired Image Trading System

RSA [13] reduces the quantization error by reducing the IR of the AOI significantly with keeping the invisibility of the AOI, however, there are rooms for improvement. The requirements for the desired image trading systems are following.

(a) *Invisible:* The most important requirement for the desired image trading system is that, the image sent to the TTP must be invisible to protect the consumer's privacy.

(b) *Low complexity:* The system complexity should be as low as possible.

(c) *High fingerprinted image quality:* The quality of fingerprinted image which is obtained by the consumer is desired to be high.

(d) *High fingerprinting performance:* While the quality of fingerprinted image is desired to be high, high fingerprinting performance which is evaluated by the correct fingerprint extracting rate, is also desired.

The next section proposes 1D transformation-based image trading system which considers these requirements.

3. PROPOSED METHODS

This section proposes 1D frequency transformation-based image trading system and distinguishes it from other IR reduction methods for AOIs.

3.1 Proposed Methods

In order to improve conventional image trading systems, 1D frequency transformation-based image trading system is proposed. Two transformations

Table 1: Processing times of 2D DFT and 1D DFT [second].

Image size	256 × 256	512 × 512	1024 × 1024
2D DFT	0.017796	0.040041	0.265450
1D DFT	0.007483	0.021167	0.096524

are considered. Firstly, 1D DFT-based image trading system is proposed as shown in Figure 6.

Let $F_c(x, v)$ be the $X \times Y$ -sized column-wise 1D DFTed coefficients of $X \times Y$ -sized image $f(x, y)$ where $x = 0, 1, \dots, X-1$, $y = 0, 1, \dots, Y-1$, and $v = 0, 1, \dots, Y-1$;

$$F_c(x, v) = \sum_{y=0}^{Y-1} f(x, y) \exp \left(-j2\pi \left(\frac{vy}{Y} \right) \right), \quad (8)$$

where j denotes $\sqrt{-1}$. DFT coefficients $F_c(x, v)$ can be expressed in the polar form as

$$F_c(x, v) = |F_c(x, v)| \exp(j\phi_c(x, v)), \quad (9)$$

where $|F_c(x, v)|$ and $\exp(j\phi_c(x, v))$ denote the amplitude and phase components of $F_c(x, v)$, respectively.

The 1D IDFT of amplitude components $|F_c(x, v)|$, which is denoted as $A_c(x, y)$, is formulated as

$$A_c(x, y) = \frac{1}{Y} \sum_{v=0}^{Y-1} |F_c(x, v)| \exp \left(j2\pi \left(\frac{vy}{Y} \right) \right), \quad (10)$$

and $A_c(x, y)$ denotes the column-wise 1D DFT-based AOI. Similarly, the POI can be defined by applying 1D IDFT to phase components $\exp(j\phi_c(x, v))$ as

$$P_c(x, y) = \frac{1}{Y} \sum_{v=0}^{Y-1} \exp(j\phi_c(x, v)) \exp \left(j2\pi \left(\frac{vy}{Y} \right) \right), \quad (11)$$

where $P_c(x, y)$ denotes the column-wise 1D DFT-based POI. It is noted that row-wise 1D DFT can also be applied instead of column-wise 1D DFT.

Similar to 2D DFT-based AOIs, 1D DFT-based AOI is invisible, and 1D DFT-based POI reveals the original image, as shown in Figs. 4 (d) and (e), respectively. Therefore, 1D DFT-based AOI satisfies the requirement (a) in Section 2.4.

The IR width of 1D DFT-based AOI is significantly lower than that of 2D DFT-based AOI. The IR and the IR width of the column-wise 1D DFT-based AOI for “Lena” are [33.1, 553.2] and 520.1, respectively. The IR width of the 1D DFT-based AOI for “Lena” is only about two times wider than that of the original image. In addition, the histogram of 1D DFT-based AOI is less skew than that of the 2D DFT-based AOI as shown in Figure 4 (g). This makes the possibility of using a linear quantization more effectively as discussed later.

The complexity of the column-wise 1D DFT for an $X \times Y$ sized image is $O((X^2)Y)$ or $O((X \log_2 X)Y)$

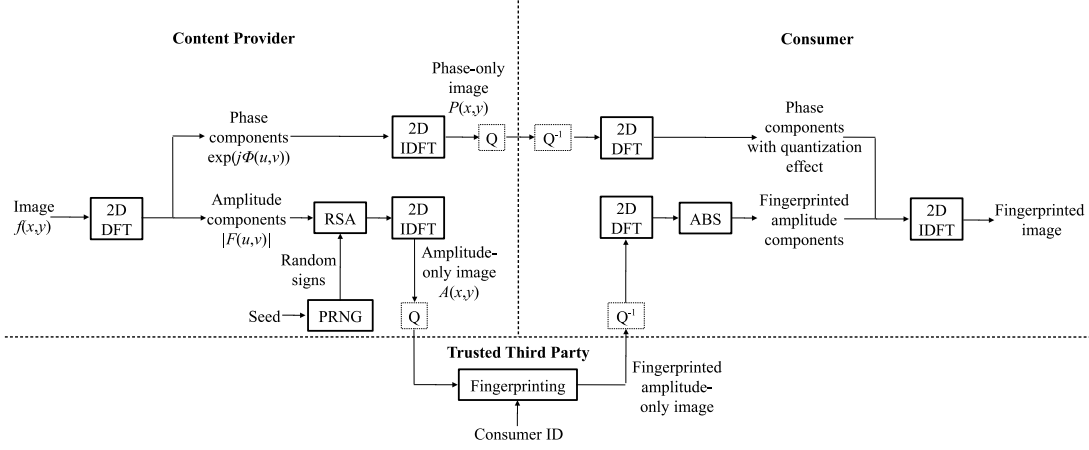


Fig.5: The image trading system using AOIs with RSA [13] (PRNG: pseudo random number generator, RSA: random sign assignment, Q : quantization, Q^{-1} : inverse quantization, and ABS: absolution).

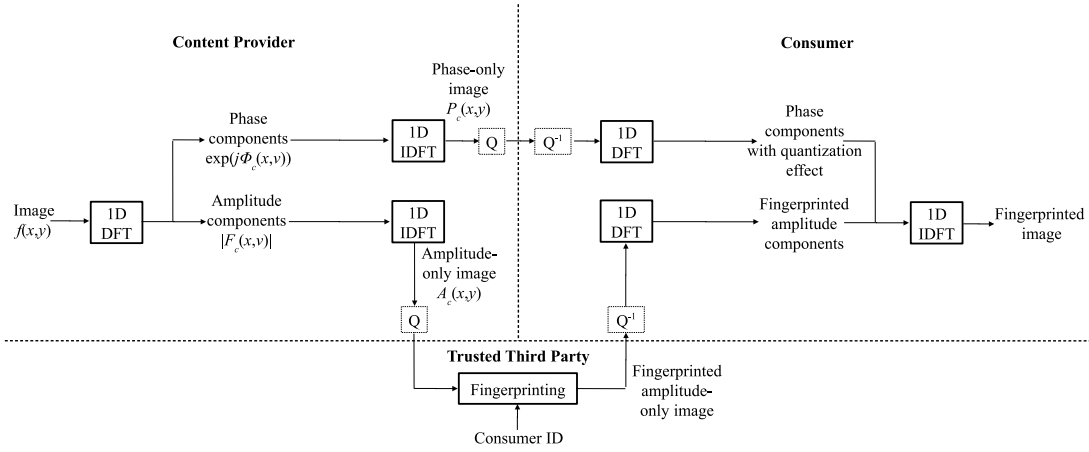


Fig.6: The proposed image trading system using 1D DFT (Q : quantization and Q^{-1} : inverse quantization).

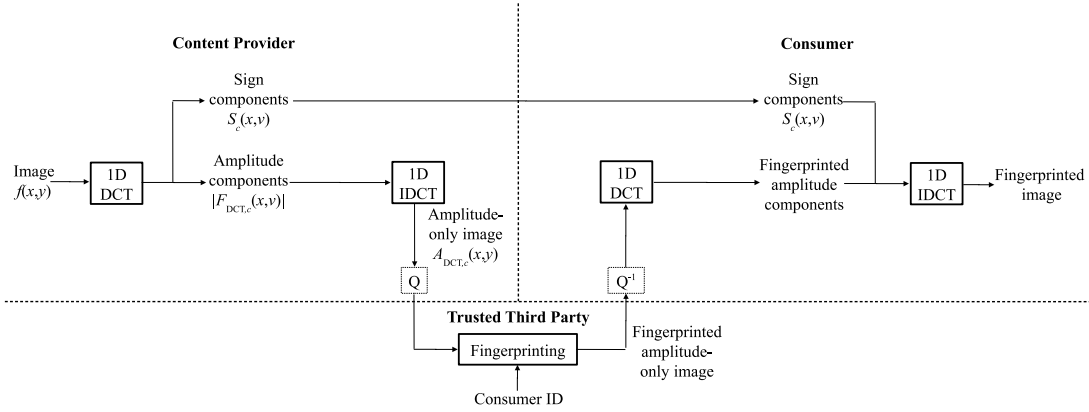


Fig.7: The proposed image trading system using 1D DCT (Q : quantization and Q^{-1} : inverse quantization).

with fast Fourier transformation (FFT), whereas that of 2D DFT is $O((XY)^2)$ or $O((XY \log_2(XY)))$ with 2D FFT. Table 1 compares the processing times of 1D DFT with those of 2D DFT for a 256×256 pixel-image, a 512×512 pixel-image, and a 1024×1024 pixel-image. The proposed 1D DFT reduces the processing time especially for large images. In addition, while RSA [13] requires extra computa-

tional costs and processing resources, the proposed 1D DFT-based method is free from such extra costs.

Secondly, 1D DCT-based image trading system which gives more advantages than 1D DFT-based image trading system is proposed as shown in Figure 7.

Let $F_{DCT,c}(x, v)$ be the $X \times Y$ -sized column-wise one-dimensional discrete cosine transformed (1D DCTed) coefficients of $X \times Y$ -sized image $f(x, y)$,

where $x = 0, 1, \dots, X - 1$, $y = 0, 1, \dots, Y - 1$, and $v = 0, 1, \dots, Y - 1$;

$$F_{\text{DCT},c}(x, v) = \sum_{y=0}^{Y-1} f(x, y) \cos \left(\frac{\pi}{Y} \left(y + \frac{1}{2} \right) v \right). \quad (12)$$

DCT coefficients $F_{\text{DCT},c}(x, v)$ can also be expressed as

$$F_{\text{DCT},c}(x, v) = |F_{\text{DCT},c}(x, v)| S_c(x, v), \quad (13)$$

where $|F_{\text{DCT},c}(x, v)|$ and $S_c(x, v)$ denote the amplitude and sign components of $F_{\text{DCT},c}(x, v)$, respectively.

The 1D IDCT of amplitude components $|F_{\text{DCT},c}(x, v)|$ can be formulated as

$$\begin{aligned} A_{\text{DCT},c}(x, y) \\ = \sum_{v=0}^{Y-1} \alpha(v) |F_{\text{DCT},c}(x, v)| \cos \left(\frac{\pi}{Y} \left(y + \frac{1}{2} \right) v \right), \end{aligned} \quad (14)$$

where

$$\alpha(v) = \begin{cases} \sqrt{\frac{1}{Y}}, & v = 0 \\ \sqrt{\frac{2}{Y}}, & v = 1, 2, \dots, Y - 1, \end{cases} \quad (15)$$

and $A_{\text{DCT},c}(x, y)$ denotes the column-wise 1D DCT-based AOI.

Distinctly from 1D DFT-based POI, sign components $S_c(x, v)$ can be stored as a binary image without performing IDCT and quantization as shown in Figure 7. It is noted that row-wise 1D DCT can also be applied instead of column-wise 1D DCT.

3.2 Advantages of The Proposed Methods

This section describes the advantages of using the proposed methods.

(A) *Using One-Dimensional Frequency Transformation:*

1D frequency transformation-based AOIs have low IRs, because 1D frequency transformation is applied to images which are 2D signals column-wise or row-wise. It could be considered that the number of the same phase cosine signals included in a single row or in a single column of the AOI in the proposed method is significantly lower than that of 2D frequency transformation-based AOI, so that the IR of the 1D frequency transformation-based AOI is much lower, viz., the number of the same phase cosine signals is reduced from XY to X column-wise or to Y row-wise. It is noted that Y iterations of a single column of the AOI generating is performed for the column-based system, and X iterations of a sin-

gle row of the AOI generating is performed for the row-based system. Without using RSA, the proposed method reduces IRs of AOIs effectively and reduces the complexity of the system. Therefore, the proposed method satisfies the requirement (b) in Section 2.4. By reducing IRs of AOIs before quantization, quantization errors of AOIs are significantly reduced. That is related to the higher quality of fingerprinted image. Therefore, the proposed method satisfies the requirement (c) in Section 2.4. In addition, obtaining the fingerprinted amplitude components to produce the fingerprinted image discards phase components of the fingerprinted AOI. This eliminates many parts of the hidden fingerprint for 2D frequency transformation-based AOIs regardless of RSA, whereas much less fingerprint is removed in 1D frequency transformation-based AOIs, because deleting 2D phase components affects much more than deleting 1D phase components. Thus, the proposed method meets requirement (d) in Section 2.4.

(B) *Using DCT Instead of DFT:* By using DCT instead of DFT, the POI generation is discarded; DCT sign components are sent from the CP to the consumer instead of the POI. A binary image is enough for storing DCT sign components perfectly. It reduces memory usage and transmission bandwidth, because if DFT is used, an 8 bpp image would be needed for storing the POI. Therefore, the proposed method satisfies requirement (b) in Section 2.4. From the different view point, DCT components are not distorted, whereas the POI is always quantized. This quantization error-free property realizes the better fingerprinted image quality, i.e., the proposed method meets requirement (c) in Section 2.4. As mentioned in the previous section, some part of the fingerprint may be lost to serve the fingerprinted image. DCT signs are two level integers, while the phase components of DFT coefficients are any arbitrary complex numbers. So, removing DFT phase components more degrades the fingerprinting performance. Thus, the proposed method satisfies requirement (d) in Section 2.4.

3.3 Other Methods to Reduce Intensity Ranges of Amplitude-Only Images

In order to distinguish the proposed method from three other IR reduction methods, BD [12], clipping, and linear scaling are described here. As shown later in experiments, these methods do not give good results compared to the proposed method.

(A) *Block Division:* One approach for reducing the IR of the AOI could be BD [12]. The IR of the AOI is reduced by dividing the original image into sub-images to reduce the number of coherent phase cosine signals in the AOI. Therefore, AOIs of sub-images are generated with low IRs. This method is similar to the proposed 1D frequency transformation-based

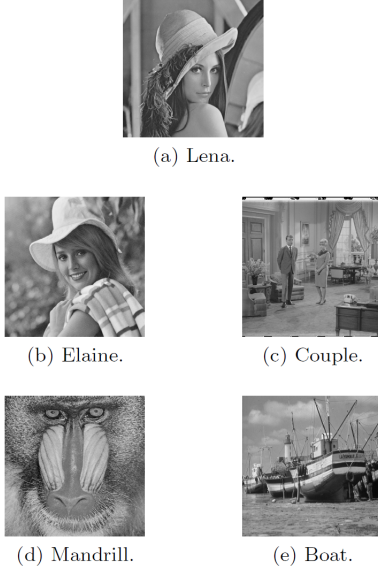


Fig.8: Test images.

system from the perspective of image dividing, however, the AOI of BD is visible when the original image is divided into many blocks. Distinctly from BD, the proposed method keeps the invisibility of the AOI.

(B) *Clipping*: Clipping could be the easiest way to reduce IRs of AOIs. It clips the IR of round ($A(x, y)$) to $[0, 2^n - 1]$, where round() returns the nearest integer, and n is the desired bit depth. With $n = 8$, numerous errors are occurred by this method.

(C) *Linear Scaling*: The intensities of AOI $A(x, y)$ are linearly scaled to $\beta A(x, y)$, where β is scaling factor. With the distribution of 2D DFT-based AOI shown in Figure 4 (f), by using a very small number of β , many low intensities disappear after linear quantization that causes numerous errors.

4. EXPERIMENTAL RESULTS

The effectiveness of the proposed method is confirmed in this section by using five test images which are “Lena,” “Elaine,” “Couple,” “Mandrill,” and “Boat” as shown in Figure 8. A simple linear quantization (LQ) is used to quantize AOIs by taking into account the entire IRs of AOIs. AOI $A(x, y)$ is quantized as

$$A_{LQ}(x, y) = \text{round}\left(\frac{A(x, y) - \min(A(x, y))}{s}\right), \quad (16)$$

$$s = \frac{\max(A(x, y)) - \min(A(x, y))}{2^n - 1}. \quad (17)$$

$A_{LQ}(x, y)$ is the quantized AOI which ranges in $[0, 2^n - 1]$, i.e., the number of quantization levels is equal to 2^n . To obtain inversely quantized AOI

$\tilde{A}(x, y)$, the inverse quantization with constant step size s and bias constant $\min(A(x, y))$ are applied to $A_{LQ}(x, y)$ as

$$\tilde{A}(x, y) = sA_{LQ}(x, y) + \min(A(x, y)). \quad (18)$$

According to the use of the LQ, the histograms of the AOIs are investigated in terms of skewness which is a measure of symmetry, because it is desired that the AOIs have the skewness near zero in order to reduce the quantization errors. A distribution is symmetric if it looks the same to the left and right of the center point. The skewness is defined as

$$\text{Skewness} = \frac{1}{XY} \sum_{i=0}^{X-1} \sum_{j=0}^{Y-1} \left(\frac{A(x, y) - \bar{A}}{\sqrt{S}} \right)^3, \quad (19)$$

where \bar{A} is the mean of $A(x, y)$, and S denotes the standard deviation of $A(x, y)$ formulated as

$$S = \sqrt{\frac{1}{XY - 1} \sum_{i=0}^{X-1} \sum_{j=0}^{Y-1} (A(x, y) - \bar{A})^2}. \quad (20)$$

The skewness for a normal distribution is zero, and any symmetrically distributed data should have a skewness near zero. Negative values for the skewness indicate that data are skewed left and positive values for the skewness indicate that data are skewed right. By skewed left, the left tail is long relative to the right tail. Similarly, by skewed right, the right tail is long relative to the left tail.

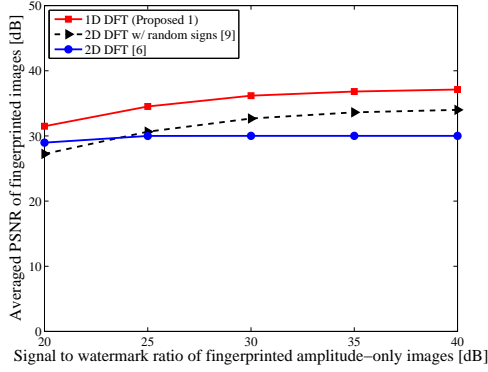
For digital fingerprinting, the block DCT-based fingerprinting technique [15] used in [6] is applied to 8 bpp LQed AOIs $A_{LQ}(x, y)$. The technique guarantees the fingerprinted image quality in terms of the signal-to-watermark ratio (SWR) by controlling the energy of the fingerprint sequence, where the SWR is given as

$$\text{SWR} = 10 \log_{10} \frac{\sum_{x=0}^{X-1} \sum_{y=0}^{Y-1} A_{LQ}^2(x, y)}{\sum_{x=0}^{X-1} \sum_{y=0}^{Y-1} \{A_{LQ}(x, y) - \hat{A}(x, y)\}^2} \quad [\text{dB}] \quad (21)$$

and $\hat{A}(x, y)$ is the fingerprinted AOI. The lower the number of desired SWR becomes, the stronger the fingerprint signal becomes. That is the fingerprint is easier to be correctly extracted when the SWR is lower. Anyway, the lower SWR of the fingerprinted AOI relates to the lower quality of the fingerprinted image reconstructed by combining the fingerprinted AOI with phase components. This trade off between the correct fingerprint extracting rate and the image quality of the fingerprinted image is general for digital fingerprinting [1].

Table 2: IR widths of AOIs.

IR width	Lena	Elaine	Couple	Mandrill	Boat
2D DFT	4819.2	4801.3	7037.0	6631.9	6438.2
2D DFT w/ RSA [13]	320.4	342.2	310.1	323.9	338.7
1D DFT	520.1	629.1	828.1	687.6	660.1
1D DCT	648.6	700.3	904.4	783.1	784.1

**Fig.9:** Averaged PSNRs of fingerprinted images where 2D DFT, 2D DFT with RSA, and 1D DFT are used for reducing IRs of AOIs.

From R which is the user-given desired SWR to be guaranteed, quantization step size Q for hiding a binary fingerprint sequence into $A_{LQ}(x, y)$ is derived as

$$Q = 10^{-0.05R} \sqrt{\frac{64}{XY} \frac{48}{7} \sum_{x=0}^{X-1} \sum_{y=0}^{Y-1} A_{LQ}^2(x, y)}. \quad (22)$$

In this section, R is varied from 20 dB to 40 dB with stepping by 5 dB. The l -th fingerprint bit w_l is hidden to low frequency AC coefficient c_l in the l -th 8×8 -sized block in the quantized AOI as

$$\hat{c}_l = Q \text{round}(c_l/Q) + w'_l, \quad (23)$$

where \hat{c}_l is the fingerprinted coefficient in the l -th block, and w'_l is the l -th energy controlled fingerprint bit given by

$$w'_l = Q(w_l - 0.5)/2 \quad (24)$$

and $l = 0, 1, \dots, L - 1$. Here, a 4096-length binary fingerprint sequence is embedded to the 512×512 -sized AOI, i.e., $L = 4096$.

Each fingerprinted AOI $\hat{A}(x, y)$ is rounded to $[0, 255]$. DFT-based POIs are linearly quantized to 8 bpp. Each fingerprinted AOI is inversely quantized by the consumer and is composed with the inversely quantized POI to obtain the fingerprinted image. In order to evaluate the quality of the fingerprinted image, it is compared with the original image in terms of peak signal-to-noise ratio (PSNR). It is noted that the fingerprinted image is rounded to $[0, 255]$ as well. In order to evaluate the fingerprinting performance, the embedded fingerprint is extracted from the rounded fingerprinted image.

Table 3: Quantization errors (MSE) of 1D DFT phases and 2D DFT phases.

MSE of phases	Lena	Elaine	Couple	Mandrill	Boat
1D DFT	0.0879	0.0910	0.1633	0.1548	0.0526
2D DFT	0.0912	0.1285	0.2011	0.2013	0.0975

4.1 Using One-Dimensional Frequency Transformation

To confirm the IR reduction performance of the proposed 1D frequency transformation-based system, column-wise 1D DFT AOIs are compared with 2D DFT-based AOIs and 2D DFT-based AOIs with RSA (seed $\sigma = 15$ for the PRNG, c.f., Figure 5).

Table 2 shows that the IR widths of the AOIs are significantly lower when 1D DFT is used instead of 2D DFT. By using 2D DFT with RSA, IR widths of AOIs are the lowest, however, extra calculations for random sign generation and multiplying signs are needed. Meanwhile, the proposed method does not need any extra calculation, instead it reduces processing resources by using 1D transformation instead of 2D transformation; memory and computational cost.

Figure 9 shows PSNRs of fingerprinted images averaged over five images where 2D DFT-based AOIs, 2D DFT-based AOIs with RSA, and 1D DFT-based AOIs are used for reducing IRs of AOIs. The results show that 1D DFT-based AOIs allow higher quality of fingerprinted images than those by other methods. Even though 1D DFT-based AOIs have a little bit wider IR widths than those by 2D DFT with RSA, higher PSNRs of 1D DFT-based fingerprinted images are obtained, because of lower quantization errors of 1D DFT phases. Table 3 shows quantization errors of 1D DFT phases and 2D DFT phases in terms of MSE.

Figure 10 shows fingerprinted images generated by using 2D DFT, 2D DFT with RSA, and 1D DFT when the desired SWR of fingerprinted AOIs = 40 dB. The results show that for 2D DFT without RSA, the visual quality of fingerprinted images is bad because of quantization errors of AOIs. 2D DFT with RSA provides better visual quality of fingerprinted images than those by 2D DFT without RSA, because RSA reduces IR widths of AOIs before quantization as shown in Table 2 so that the quantization errors are reduced. The use of 1D DFT provides as good visual quality of fingerprinted images as the 2D DFT with RSA, and it does not effect the coherency of the reconstructed image, even though the 1D transformation-based AOI is lack of the inter-column or inter-row relationship. Since the transformation is reversible, the coherency of the reconstructed image is preserved.

Figure 11 shows averaged correct fingerprint extracting rates. The results also show that 1D DFT-based AOIs allow higher correct fingerprint extracting rates than those by 2D DFT-based AOIs and 2D DFT-based AOIs with RSA.

It is concluded from these results that using a 1D

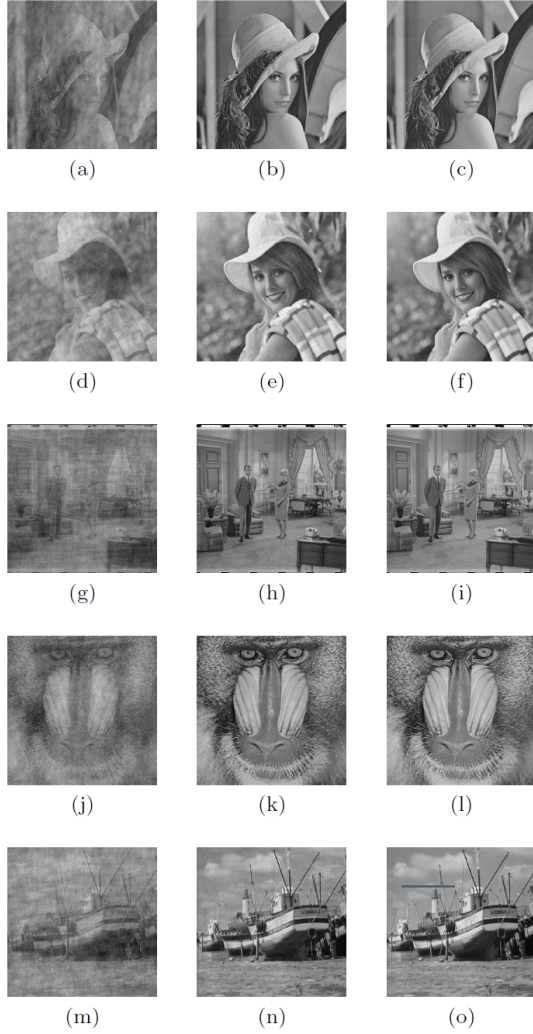


Fig.10: Fingerprinted images when the desired SWR of fingerprinted AOIs = 40 dB. The left column: 2D DFT. The middle column: 2D DFT with RSA. The right column: 1D DFT. The first row, the second row, the third row, the fourth row, and the fifth row: Lena, Elaine, Couple, Mandrill, and Boat, respectively.

transformation instead of a 2D transformation contributes not only to IR reduction and AOI generating cost reduction but also to the quality of fingerprinted images and fingerprinting performance.

4.2 Using DCT Instead of DFT

To confirm the effectiveness of using DCT-based AOI, 1D DCT-based AOIs are compared with 1D DFT-based AOIs. IR widths of 1D DCT-based AOIs are shown in Table 2. Even though they are slightly higher than those of 1D DFT-based AOIs, the qualities of 1D DCT-based fingerprinted images are higher than those of 1D DFT-based as shown in Figure 12, because DCT sign components are handled perfectly by binary images.

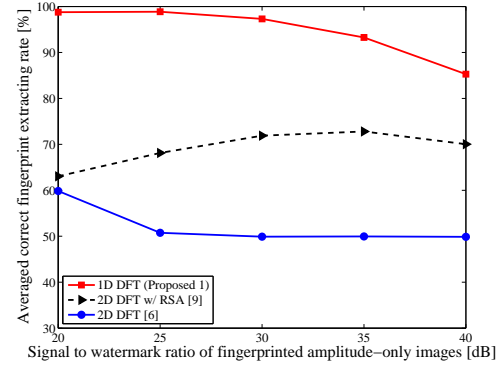


Fig.11: Averaged correct fingerprint extracting rates where 2D DFT, 2D DFT with RSA, and 1D DFT are used for reducing IRs of AOIs.

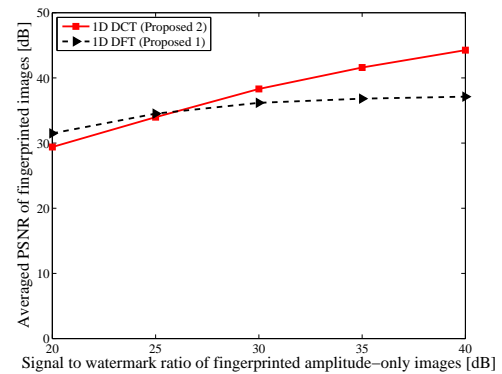


Fig.12: Averaged PSNRs of fingerprinted images where 1D DFT AOI and 1D DCT are used for reducing IRs of AOIs.

It is concluded from these results that using DCT-based AOIs instead of DFT-based AOIs improves the image quality of fingerprinted images.

Figure 13 shows averaged correct fingerprint extracting rates. The results show that when using DCT, higher correct fingerprint extracting rates are also obtained.

4.3 Others Methods to Reduce Intensity Ranges of Amplitude-Only Images

BD [12], Clipping, and linear scaling are evaluated in this part. For BD, each original image is divided into sub-images before generating AOIs of sub-images independently with various block sizes. Figure 14 shows BD-based AOIs. The results show that BD can reduce IRs of AOIs significantly. However, invisibility of AOIs is destroyed by too small block sizes. With the acceptable block sizes that keep the AOIs invisible, IRs of AOIs cannot be reduced as good as those in the proposed method. So, BD is not suitable for the copyright- and privacy-protected image trading system.

For clipping, 2D DFT-based AOIs are clipped to [0, 255] and rounded to integers to be stored in 8 bpp before fingerprinting. For linear scaling, each scaling

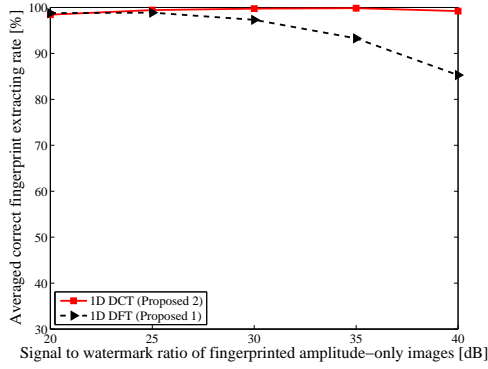


Fig.13: Averaged correct fingerprint extracting rates where 1D DFT and 1D DCT are used for reducing IRs of AOIs.

Table 4: Conclusions of effectiveness of considered methods (C_1 : 2D DFT [6], C_2 : 2D DFT with RSA [6], P_1 : 1D DFT (Proposed 1), P_2 : 1D DCT (Proposed 2), BD: block division [12], CP: clipping, and LS: linear scaling).

Requirement	C_1	C_2	P_1	P_2	BD	CP	LS
(a)	○	○	○	○	×	○	○
(b)	△	△	○	○	-	△	△
(c)	×	○	○	⊙	-	×	×
(d)	△	△	○	⊙	-	△	△

factor is calculated for each 2D DFT-based AOI to store them in 8 bpp as follows.

$$\beta = \frac{2^n - 1}{\max(A(x, y))}, \quad (25)$$

where β denotes scaling factor, and $n = 8$ here. With rounding, the scaled AOI $A_{scale}(x, y)$ can be calculated as

$$A_{scale}(x, y) = \text{round}(\beta A(x, y)). \quad (26)$$

Therefore, $A_{scale}(x, y)$ ranges in $[0, 255]$. In order to obtain the re-scaled AOI, the scaled AOI is divided by the scaling factor β . For both methods, POIs are linearly quantized to 8 bpp.

Figure 15 shows PSNRs of fingerprinted images averaged over five images where clipping and scaling are used for reducing IRs of AOIs. The results show that both clipping and linear scaling are not effective methods. They give much lower PSNRs of fingerprinted images comparing with those by the proposed method. Figure 16 shows averaged correct fingerprint extracting rates. The results show that clipping and linear scaling also give much lower correct fingerprint extracting rates comparing with those by the proposed method.

By above results, the effectiveness of all considered methods could be concluded as Table 3, where C_1, C_2, P_1, P_2 , BD, CP, and LS denote 2D DFT-based image trading system (conventional 1) [6], 2D DFT with RSA-based image trading system (conventional 2) [13], 1D DFT-based image trading system (proposed 1), 1D DCT-based image trading system (proposed 2), BD-based image trading system [12], clipping-based image trading system, and linear scaling-based image trading system, respectively.

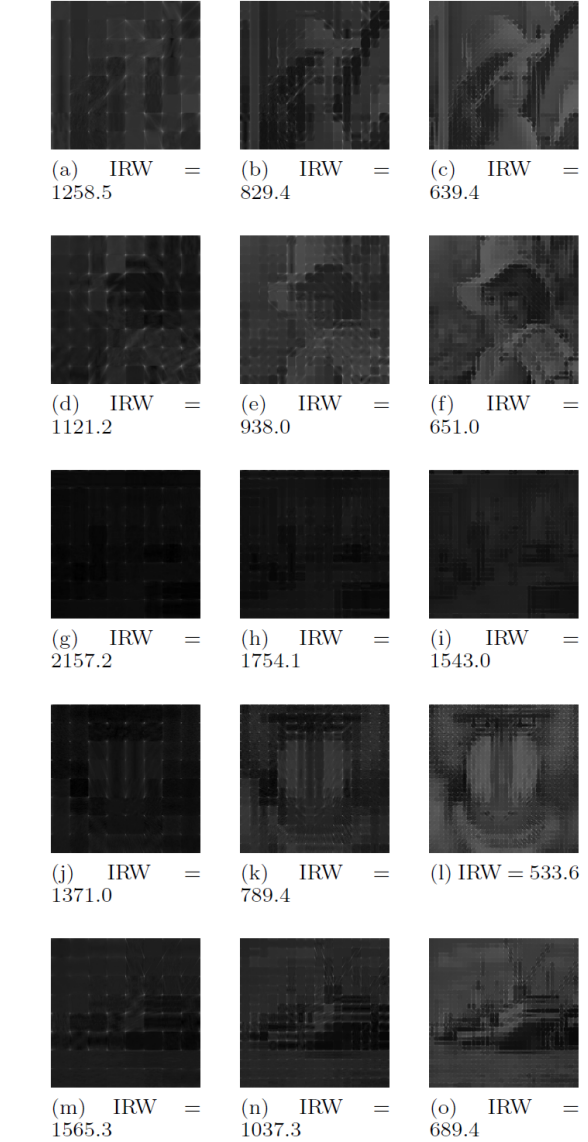


Fig.14: Block division-based AOIs. The left column: 64×64 pixels per block. The middle column: 32×32 pixels per block. The right column: 16×16 pixels per block. The first row, the second row, the third row, the fourth row, and the fifth row: Lena, Elaine, Couple, Mandrill, and Boat, respectively. IRW: intensity range width.

tem (proposed 1), 1D DCT-based image trading system (proposed 2), BD-based image trading system [12], clipping-based image trading system, and linear scaling-based image trading system, respectively. Requirements (a), (b), (c), and (d) are those described in Section 2.4. Symbols “×,” “△,” “○,” and “⊙” mean “bad,” “fair,” “good,” and “excellent,” respectively.

As shown in Table 5, the skewness of the scaled AOI is as high as the skewness of the 2D DFT-based AOI. This is confirmed that the linear scaling method does not work well. It only reduces the intensity

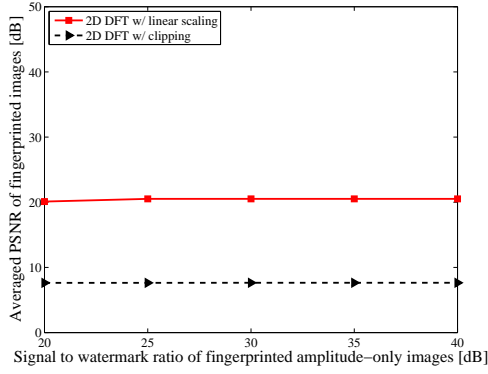


Fig.15: Averaged PSNRs of fingerprinted images where clipping and linear scaling are used for reducing IRs of AOIs.

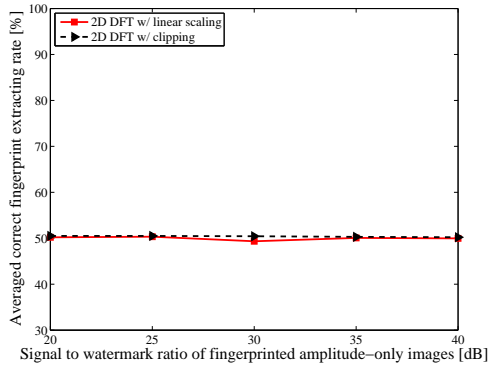


Fig.16: Averaged correct fingerprint extracting rates where clipping and linear scaling are used for reducing IRs of AOIs.

range of the AOI without considering the histogram of the AOI. Even though clipping gives much lower skewness, numerous errors are introduced, because this method is non-reversible. As same as the original image and the RSA-based AOI, the proposed 1D frequency transformation-based AOIs have near zero skewness.

5. CONCLUSIONS

This paper has proposed an effective method of AOI generation based on 1D frequency transformation. The proposed method reduces the IR of AOIs comparably to RSA [13] and reduces the computational resources as well. In addition, DCT-based image trading system has been proposed in this paper to enhance the quality of the fingerprinted image. The results show that the proposed method is superior to the conventional methods [6, 13] in terms of quality of fingerprinted images and fingerprinting performance. It concludes that the proposed method makes the copyright- and privacy-protected image trading system [4-16, 12-14] more practical.

Table 5: Skewness of histograms of AOIs for “Lena.”

Image	Skewness
Original image	-0.0282
2D DFT-based AOI	18.7145
2D DFT-based AOI w/ RSA	0.1051
1D DFT-based AOI	2.3758
1D DCT-based AOI	2.3792
Clipped AOI	2.0029
Linear scaled AOI	18.2834

ACKNOWLEDGMENT

This work has been partially supported by the Grand-in-Aid for Scientific Research (C), No.24560468, from the Japan Society for the Promotion of Science.

References

- [1] I.J. Cox, M.L. Miller, J.A. Bloom, J. Fridrich, and T. Kalker, “Digital watermarking and steganography,” 2nd ed., *Morgan Kaufmann Publishers*, 2008.
- [2] M. Kuribayashi, “Recent fingerprinting techniques with cryptographic protocol,” *Signal Processing*, S. Miron, ed., *InTech*, 2010.
- [3] B. Schneier, “Applied cryptography: protocols, algorithms, and source code in C,” 2nd ed., *John Wiley & Sons*, 1996.
- [4] M. Okada, Y. Okabe, and T. Uehara, “A web-based privacy-secure content trading system for small content providers using semi-blind digital watermarking,” *Proc. IEEE CCNC*, 2010.
- [5] Y. Sengoku and H. Hioki, “An image segmentation method for privacy and copyright-aware image trading system,” *IEICE Tech. Rep.*, vol.111, no.496, EMM2011-67, pp.19–24, Mar. 2012.
- [6] S. Liu, M. Fujiyoshi, and H. Kiya, “An image trading system using amplitude-only images for privacy- and copyright-protection,” *IEICE Trans. Fundamentals*, vol.E96-A, no.6, pp.1245–1252, Jun. 2013.
- [7] K. Takita, T. Aoki, Y. Sasaki, T. Higuchi, and K. Kobayashi, “High-accuracy subpixel image registration based on phase-only correlation,” *IEICE Trans. Fundamentals*, vol.E86-A, no.8, pp.1925–1934, Aug. 2003.
- [8] I. Ito and H. Kiya, “One-time key based phase scrambling for phase-only correlation between visually protected images,” *EURASIP J. Inf. Security*, vol.2009, no.841045, Jan. 2010.
- [9] I. Ito and H. Kiya, “Phase-only correlation based matching in scrambled domain for preventing illegal matching,” *LNCS Trans. Data Hiding and Multimedia Security V*, vol.6010/2010, pp.51–69, Jun. 2010.
- [10] C.A. Wilson and J.A. Theriot, “A correlation-based approach to calculate rotation and translation of moving cells,” *IEEE Trans. Image Process.*, vol.15, no.7, pp.1939–1951, Jul. 2006.

- [11] A.V. Oppenheim and J.S. Lim, "The importance of phase in signals," *Proc. IEEE*, vol.69, pp.529–541, May. 1981.
- [12] W. Sae-Tang, M. Fujiyoshi, H. Kobayashi, and H. Kiya "Intensity range reduction of amplitude-only images," *Proc. IWAIT*, pp.322–327, Jan. 2013.
- [13] W. Sae-Tang, M. Fujiyoshi, and H. Kiya, "A Generation Method of Amplitude-Only Images with Low Intensity Ranges," *IEICE Trans. Fundamentals*, vol.E96-A, no.6, pp.1323–1330, Jun. 2013.
- [14] W. Sae-Tang, M. Fujiyoshi, and H. Kiya, "An Intensity Range Reduction Method for the Image Trading System with Digital Fingerprinting in Visually Protected Domain," *IEEE ISCIT 2013*, pp.423–428, Sep. 2013.
- [15] T. Tachibana, M. Fujiyoshi, and H. Kiya, "A watermarking scheme retaining the desired image quality in order to be applicable to watermarks with various distributions," *IEICE Trans. Inf. & Sys. (Japanese Edition)*, vol.J87-D-II, no.3, pp.850–859, Mar. 2004.



Wannida Sae-Tang received her B.Eng. degree in Electronic and Telecommunication Engineering with the first class honor and her M.Eng. degree in Electrical Engineering from King Mongkut's University of Technology Thonburi, Thailand in 2007 and 2011, respectively. From 2007 to 2009, she was an IC packaging design engineer of New product design and research and development team at United Test and Assembly Center Thai Ltd. Currently, she is a Ph.D. student of Information and Communication Systems at Tokyo Metropolitan University with Tokyo metropolitan governmental Asian human resources fund. Her research interests include image processing and multimedia communication. She received the Best Paper Award of the IEICE/ITE/KSBE IWAIT in 2014. She is a student member of the IEEE and IEICE.

ter Thai Ltd. Currently, she is a Ph.D. student of Information and Communication Systems at Tokyo Metropolitan University with Tokyo metropolitan governmental Asian human resources fund. Her research interests include image processing and multimedia communication. She received the Best Paper Award of the IEICE/ITE/KSBE IWAIT in 2014. She is a student member of the IEEE and IEICE.



IEICE.

Shenchuan Liu received his B.Eng. degree in electrical engineering from Dalian University of Technology, China in 2006 and his M.Eng. from Tokyo Metropolitan University, Japan in 2011, respectively. He is currently a Ph.D. student of Information and Communication Systems at Tokyo Metropolitan University. His research interests include image processing and multimedia security. He is a Student Member of the IEEE and



the IEICE in 2001. He is a Member of the IEEE, EURASIP, APSIPA, IEICE, and ITE.

Masaaki Fujiyoshi received his Ph.D. degree from Saitama University, Japan in 2001. In 2001, he joined Tokyo Metropolitan University, Japan, where he is currently an Assistant Professor. His research interests include image processing, multimedia security, and spread spectrum communications. Dr. Fujiyoshi served as an Associate Editor of the J. IEICE from 2005 to 2007. He received the Young Engineer Award from the IEICE in 2001. He is a Member of the IEEE, EURASIP, APSIPA, IEICE, and ITE.



Hitoshi Kiya received his B.Eng. and M.Eng. degrees from Nagaoka University of Technology, Japan, in 1980 and 1982 respectively, and his Dr.Eng. degree from Tokyo Metropolitan University in 1987. In 1982, he joined Tokyo Metropolitan University as an Assistant Professor, where he became a Full Professor in 2000. From 1995 to 1996, he attended the University of Sydney, Australia as a Visiting Fellow. He currently

serves as the Chair of IEEE SPS Japan Chapter, an Associate Editor of IEEE Trans. Image Processing and of IEEE Trans. Information Forensics and Security, respectively. He also served as the President of IEICE ESS, an Associate Editor of IEEE Trans. Signal Processing, the Editor-in-Chief of IEICE Fundamentals Review, a Vice President of APSIPA, a Member of the Board of Governors of APSIPA, and the Publications Board Chair of IEICE ESS. His research interests are in the area of signal and image processing including multirate signal processing, wavelets, video coding, compressed-domain video manipulation and security for multimedia. He received the ITE Niwa-Takayanagi Best Paper Award in 2012, the Telecommunications Advancement Foundation Award in 2011, the IEICE ESS Contribution Award in 2010, and the IEICE Best Paper Award in 2008. He is a Fellow Member of the IEICE and ITE, and he is also a Senior Member of the IEEE.